ilmedia

TECHNISCHE UNIVERSITÄT ILMENAU

Hofmann, Martin; Holz, Mathias; Plank, Harald; Strehle, Steffen

Localized direct material removal and deposition by nanoscale field emission scanning probes

Original published in: Micro and nano engineering. - Amsterdam : Elsevier. - 16 (2022), p. 1-5.

Original published: 2022-05-18

ISSN: 2590-0072

DOI: 10.1016/j.mne.2022.100146

[*Visited:* 2022-09-26]

This work is licensed under a Creative Commons Attribution 4.0 International license. To view a copy of this license, visit https://creativecommons.org/licenses/by/4.0/

TU Ilmenau | Universitätsbibliothek | ilmedia, 2022
http://www.tu-ilmenau.de/ilmedia

MNE 16 (2022) 100146

Contents lists available at ScienceDirect

Micro and Nano Engineering

journal homepage: www.sciencedirect.com/journal/micro-and-nano-engineering

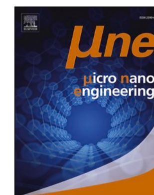

Localized direct material removal and deposition by nanoscale field emission scanning probes

Martin Hofmann [a], Mathias Holz [a], Harald Plank [b], Steffen Strehle [a,*]

[a] Technische Universität Ilmenau, Institute of Micro- and Nanotechnologies MacroNano®, Microsystems Technology Group, Max-Planck-Ring 12, 98693 Ilmenau, Germany

[b] Christian Doppler Laboratory for Direct-Write Fabrication of 3D Nano-Probes, Institute of Electron Microscopy and Nanoanalysis, Graz University of Technology, Steyrergasse 17, 8010 Graz, Austria

A R T I C L E I N F O

Keywords:
Electron beam induced processing
Scanning probe
Removal
Etching
Deposition
Field-emission

A B S T R A C T

The manufactory of advanced micro- and nanoscale devices relies on capable patterning strategies. Focused electron beams, as for instance implemented since long in electron beam lithography and electron beam induced deposition, are in this regard key enabling tools especially at the early stages of device development and research. We show here that nanoscale field emission scanning probes can be potentially utilized as well for a prospective direct device fabrication by localized material deposition but notably, also by localized material removal. Field emission scanning probe processing was specifically realized on 10 nm chromium and 50 nm gold thin film stacks deposited on a (1×1) cm^2 fused silica substrate. Localized material deposition and metal removal was studied in various atmospheres comprising high vacuum, nitrogen, ambient air, naphthalene and carbon-dioxide. Stable and reliable regimes were in particular obtained in a carbonaceous atmosphere. Hence, localized carbon deposits were obtained but also localized metal removal was realized. We demonstrate furthermore that the selected electron emission parameters (20 V - 80 V, 180 pA) and the overall operation environment are crucial aspects that determine the degree of material deposition and removal. Based on our findings, direct tip-based micro- to nanoscale material patterning appears possible. The applied energy regime is also enabling new insights into low energy (< 100 eV) electron interaction. However, the underlying mechanisms must be further elucidated.

1. Introduction

From today's perspective, a series production of devices in the scale of only a few atoms is within reach [1]. However, an important prerequisite for the efficient fabrication of novel and advanced nano- and microstructured devices is the reproducible generation of functional structures in the respective length scale, which also includes the third dimension. New and unconventional patterning and analyzing tools with high performances are therefore essential as key technologies that ideally enable patterning and analysis resolution adoptable from the micro- down to the nanometer scale. Scanning probe microscopy (**SPM**) technologies are in this regard extremely powerful. SPM techniques were developed to observe physical, chemical or biological interactions between a sharp tip and a sample surface. Common tip apex radii are in the range of several tens of nanometers down to the single nanometers scale. A well-known representative of SPM is the atomic force microscope (**AFM**). Here, intermolecular attractive and repulsive forces create an interaction between a miniaturized probe tip and a substrate, which are detected and used to reconstruct, for instance, the substrate surface topography. The close proximity down to the sub-nanometer range between the sharp probe and the substrate surface yields a spatially and highly confined nanoscale interaction region. Hence, it became possible to push the scientific progress towards nanometer scales in many research areas [2]. In this so-called imaging mode, manipulation of the specimen is in principle not intended. However, aside from microscopy, scanning probes can be used as well for the nanoscale patterning of surfaces [3]. Various kinds of tip-sample interactions, such as mechanical, thermal, electrical and diffusive interactions, can result in a localized material removal as well as in deposition under special conditions. Ultimatly, the true strength of scanning probe techniques emerges from the controlled capability to switch between non-destructive nanoscale imaging and destructive

* Corresponding author.
E-mail address: steffen.strehle@tu-ilmenau.de (S. Strehle).

https://doi.org/10.1016/j.mne.2022.100146
Received 7 March 2022; Received in revised form 4 May 2022; Accepted 14 May 2022
Available online 18 May 2022
2590-0072/© 2022 The Authors. Published by Elsevier B.V. This is an open access article under the CC BY license (http://creativecommons.org/licenses/by/4.0/).

patterning mode without the requirement of a probe or even system exchange. A sequential read/write cycle allows in-situ surface inspection before and after scanning probe patterning and enables precise pattern overlay alignment and also stitching. Using scanning probe lithography, such as field emission scanning probe lithography (**FE-SPL**) and thermal scanning probe lithography (**t-SPL**), features in the sub-20 nm regime and even below were successfully created [4–7].

However, ultra-thin resist layers (thickness < 20 nm) must be utilized to achive high-resolution nanoscale lithographic patterning, while considering requirements set by the subsequent processing, such as dry-etching or lift-off procedures. Therefore, these techniques actually only support the creation of so-called 2.5-dimensional nanostructures with precise morphology and shape control in the plane, but very limited control in the third dimension. To push the current technological possibilities in future beyond these limitations, while simultaneously widening the scope of materials would enable new design and fabrication strategies for numerous nanoscale devices.

With respect to our research presented here, the starting point for the development in such a direction are electron- and field-induced reactions of gaseous precursors that are established within focused electron beam induced processing (**FEBIP**) [9,10]. They also support the direct-write fabrication of even complex 3D nanoscale structures from various materials by localized additive and subtractive processes based on an occuring precursor gas decomposition. Although powerful in its capabilties, FEBIP approaches indispensably require high-vacuum conditions for reliable operation. In contrary, scanning probe techniques can be operated under ambient and, in principle, even in various precursor gas atmospheres and pressure regimes. In this regard, Garcia et al. showed recently that carbonaceous sub-25 nm dots can be created on a silicon substrate using so-called oxidation SPL in a CO_2 environment [11]. Expensive and time-consuming vacuum systems, as for instance necessary for scanning electron microscopy (**SEM**), can therefore be omitted. Here, we demonstrate first results of so-called tip-based electron beam induced (**TEBI**) processing by field emission scanning probes as similarly used for FE-SPL. A schematic illustration of TEBI processing is shown in Fig. 1a. In dependence on the overall electron emission characteristics, the choice of precursor gas, and the utilized substrate material, localized material deposition from decomposed precursor molecules (left) as well as localized material removal (right) are conceivable. We demonstrate a deposition but notably as well a direct removal of material, here mainly the metal gold, by TEBI structuring in a carbonaceous atmosphere.

2. Methods

In this research work, we employed an AFM that was in-built into a SEM, called AFMinSEM (nano analytik GmbH, Germany) []. This system enabled TEBI processing and direct SEM inspection of the sample surface [8,12]. The AFMinSEM tool (Fig. 1b and c) was installed into a FIB/SEM microscope (Helios NanoLab 600i) from Thermo Fisher Scientific. The AFM was equipped with active cantilevers that allow a precise thermomechanical actuation near the sample surface combined with a piezoresistive read-out of the microcantilever deflection. For navigation and coarse positioning, a motorized *XYZ*-stage is used that can address an area of up to (18 × 18 × 10) mm^3 with a resolution of 1 nm. High-resolution metrology and nanofabrication can be carried out using a bottom *XYZ*-capacitive-closed-loop-scanner. Thus, it is possible to image an area of (60 × 60 × 20) μm^3 with a resolution of 0.4 nm in *X* and *Y* and 0.2 nm in *Z*. The use of active cantilevers enables the implementation of two independent scanning probe methods in a single setup. Here, we combine the two scanning probe methods AFM for surface imaging and, in principle, FE-SPL for patterning. For the FE-SPL mode, a bias voltage that is applied between probe tip and the sample generates an electric field that is naturally enhanced in the vicinity of the ultra-sharp conductive tip apex [13]. The confined electric field triggers an emission of low energy electrons, which are ideal for chemical precursor dissociation in the range of a few eV [14]. The tool allows a bias voltage tuning up to 100 V and an emission current set-point of up to 200 pA. The interaction of both parameters influences the distance control of the tip-sample distance and consequently the overall achievable line width. Under ideal conditions, writing speeds up to 10 μm/s can be achieved. As proper operation requires an electrically conductive sample at ground potential, our TEBI experiments were performed on thin film stacks consisting of 10 nm chromium followed by 50 nm gold, fabricated via electron beam evaporation on 1 × 1 cm^2 fused silica substrates. Naphthalene ($C_{10}H_8$) was used, as it is an already well-established precursor for electron beam induced carbon deposition [11]. Gas delivery was done with a conventional gas injection system (**GIS**), evident in Fig. 1c, which was mounted in an inclination angle of 30° relative to the surface, a radial distance of about 150 μm to the AFM tip and substrate. For TEBI experiments, naphthalene was heated up to 32 °C at least 1 h prior to deposition, while the GIS valve was opened for 5 min prior to

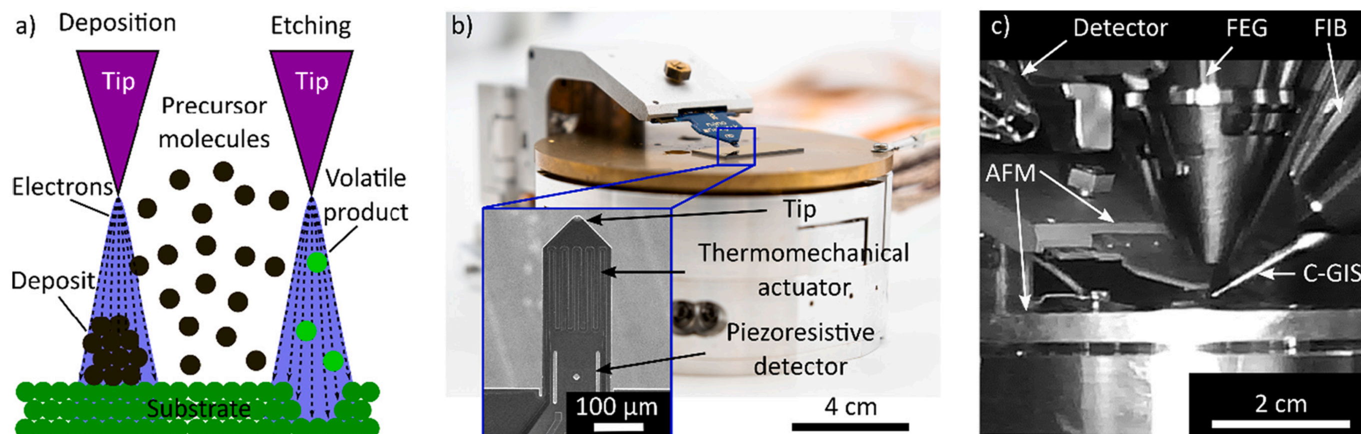

Fig. 1. a) Schematic illustration of tip-based electron beam induced (TEBI) processing by means of deposition and removal at the left and right, respectively. Due to electron induced precursor gas molecule decomposition, non-volatile species yield a localized deposit on the substrate surface, while reactive species should trigger localized material removal. b) Optical image of the utilized AFMinSEM tool [8]. The magnified view (SEM image) shows the utilized field emission active microcantilever in detail. c) Optical image of the AFMinSEM tool as installed in a dual beam system. Both tools complement each other. Using the field emission gun (FEG) and dedicated read-out, one can identify a region of interest on a sample by SEM and subsequently perform AFM at sub-nm-resolution. Furthermore, naphthalene precursor molecules can be injected into the same sample region using a conventional SEM gas injection system (GIS). The system is additionally equipped with a gallium focused ion beam (FIB) that was not used in this study.

any TEBI experiments to ensure a thermodynamic equilibrium between adsorption and desorption. During that procedure, the background vacuum of 2.3×10^{-4} Pa increased to 7.5×10^{-3} Pa under full saturation. Further experiments were carried out in nitrogen (N_2) and carbon dioxide (CO_2) atmosphere at ambient pressure as well as in ambient air conditions. The created deposits were primarily analyzed by SEM, using 10 keV and 86 pA in top and tilted views but also via AFM and energy dispersive X-ray spectroscopy (**EDX**) at 10 keV and minimal currents to obtain acceptable signal-to-noise ratios. In all experiments, emission currents and writing speeds were kept constant at 180 pA and 0.05 μm/s, respectively using probes with a tip radius of about 60 nm. Parallel line features were generated using with a single line being 20 μm long and a line interspacing of 5 μm. The applied bias voltage was increased at each line from 20 V to 80 V with an increment of 10 V. In order to maintain an emission current of 180 pA, the tip to sample distance is varied.

3. Results and discussion

The first TEBI processing experiments were realized under high vacuum conditions to create reference experiments without any precursor gas usage. As evident in Fig. 2a, material deposition was still observed, presumably from electron-induced decomposition of residual carbonaceous molecules from the background vacuum but in particular from the substrate itself from naturally present surface contaminations due to ambient transfer from preparation to TEBI instrumentation. Similar carbonaceous deposits are well-known from conventional SEM imaging as described elsewhere [15]. From Fig. 2a it becomes evident that the deposited carbon features smear out increasingly at higher bias voltage and are barely visible anymore at bias voltages above 60 V. This effect of so-called line smearing is already known in comparable manner for the FE-SPL exposure of ultra-thin electron-sensitive calixarene resist [16].

Gas molecules can generally interact with an electron beam, especially in the case of low energy electrons as used in this study. To investigate the general pressure dependency of the process, nitrogen was implemented at ambient pressures, while TEBI experiments were done with identical settings. In comparison to features that were deposited under vacuum (cf. Fig. 2a), fine and well distinguishable line patterns are now detectable at the substrate surface (Fig. 2b). The responsible mechanisms for the observed feature enhancement are so far not clear.

To trigger a carbon deposition, the concentration of carbonaceous species, such as volatile hydrocarbons and CO_2, was subsequently increased by replacing gaseous nitrogen with air but keeping the ambient pressure of about 10^5 Pa. A respective SEM image is illustrated in Fig. 2c). Despite an expected increase in localized carbon deposition, line patterns are barely visible for bias voltages of 20 V to 30 V and exhibit a more delicate morphology in comparison to the deposits achieved in nitrogen atmosphere.

Besides the demonstrated material deposition due to gas decomposition, other effects must be consequently also considered. First, adsorbed water layers due to air moisture might impair the electron surface interaction and second, material removal effects might occur as well. The removal of material from the surface could emerge, for instance, from chemical etching decomposed gas molecules, radicals and gaseous ions and also ablative discharge effects can be in principle discussed. Oxygen radicals and ions might etch in this regard, for instance, deposited carbon due to an occurring chemical reaction that might yield

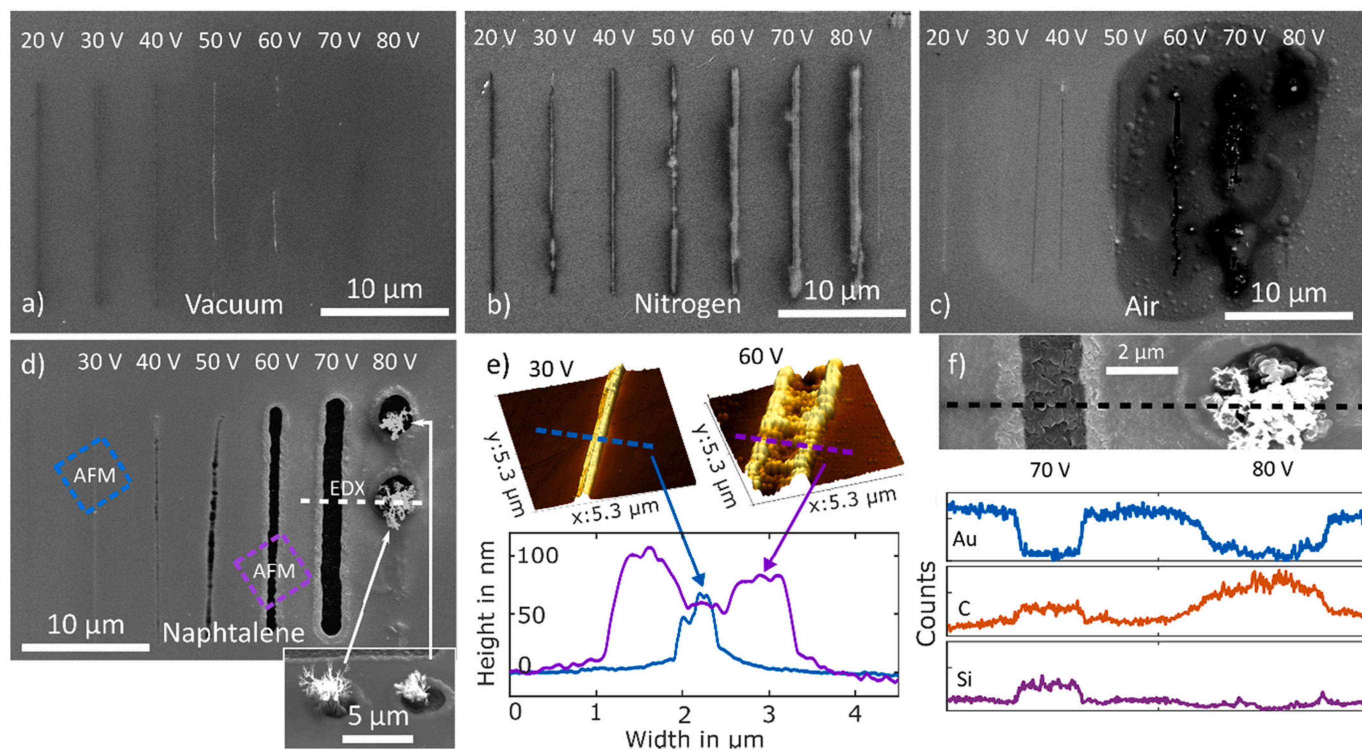

Fig. 2. Sample surface images after TEBI processing (electrical emission current and writing speed were 180 pA and 0.05 μm/s, respectively) using various atmospheres as indicated. Line patterns (line length 20 μm) were generated with a bias voltage of 20 V to 80 V (increment 10 V).: a) vacuum environment (10^{-4} Pa; working base pressure of the SEM), b) nitrogen environment at about 10^5 Pa pressure, c) ambient air environment, d) GIS created naphthalene environment, e) AFM surface reconstruction of two line sections created with 30 V and 60 V bias voltage in a naphthalene environment as well as illustration of the respective feature cross-sections. Scanned areas are indicated by dashed squares in d). Total line widths from about 0.5 μm at 30 V to 2.2 μm at 60 V can be detected (measured as full width at half maximum). f) SEM/EDX analysis line scan of created features by TEBI processing with the naphthalene precursor. The line scan was carried out at sample positions as indicated in d). The counts axis is the same for all elements. The deposition of carbon but also the removal of the metal gold is evidently shown. (For interpretation of the references to colour in this figure legend, the reader is referred to the web version of this article.)

volatile CO_2. Aside from changes in the deposition rate and line pattern morphology, substrate material removal might notably occur in air at an applied bias voltage of 60 V (Fig. 2c). Nevertheless, these potentially etched features exhibit additionally coronas of dark appearance that broaden with increasing bias voltage, which implies a broadened carbon deposition or gold roughening rather than material removal. An increase in surface roughness and bubble formation or local delamination of the surrounding metal layer also develops simultaneously.

Localized and direct TEBI material removal would be an intriguing and powerful tool enabling new degrees of freedom in micro- and nanoscale device fabrication. However, elucidation and clarification of the general occurrence of TEBI surface deposition and removal regimes require further experiments. To exclude primarily moisture and oxygen, TEBI experiments were realized under high-vacuum conditions but this time with naphthalene as precursor gas, locally injected by the GIS. Despite an expected significant increase in the local carbon concentration during TEBI processing, barely any carbon containing features (dark areas) are apparent in the voltage range from 30 V to 80 V (Fig. 2d).

This aspect differs significantly in comparison to the aforementioned vacuum-only experiments (Fig. 2a) that suggested carbon deposition for such low voltages. Notably, for TEBI processing bias voltages in the range of 40 V to 70 V, the impression is again created that substrate surface modification occurred. Nevertheless, for a set bias voltage of 80 V, the potential surface modification effect is clearly interfered by a material deposition, which results in our experiments in a formation of carbonaceous structures (Fig. 2d). SEM inspection in combination with sample tilting revealed tree-like feature growth.

To clarify the question on how TEBI processing modification occurs, AFM measurements were done as shown in Fig. 2e for patterns created in a naphthalene atmosphere. The AFM images show clearly that deposits rather than etched pits were created during TEBI processing. TEBI experiments at a bias voltage of 30 V yield in this regard about 500 nm wide deposited lines with a height of about 70 nm. The lines are notably larger than the scanning tip radius, which is in the range of 60 nm. Increasing the bias voltage yields a clear broadening of the features and demonstrates that the process can indeed be controlled. Line patterns that were created with a bias voltage of 60 V showed a line width of already 2.2 μm and a maximum height of about 100 nm at the edge regions of the M-shaped cross-sectional shape (discussed later in more detail).

To evaluate the composition of the modified sample surface for the lines (70 V bias) and the 3D deposits (80 V bias), EDX line scans were performed as shown in Fig. 2f. The first detail is the decreasing gold signal (blue curve) at the location of the line feature, which is accompanied by an increase in silicon (purple), which is to be expected with an etched gold layer on silicon. However, the carbon signal is also increasing (orange curve), which strongly suggests deposition of naphthalene and/or contamination from the surface/vacuum. Hence, it seems that we have two concurrent processes at the same time: carbon deposition and gold removal, which at 70 V are dominated by the latter one.

Another detail of relevance, which supports the aforementioned hypothesis of roughening or removing gold by an electron-beam induced process in the presence of carbon, is the fact that the gold signal is not varying at taller edge regions at the 70 V line (see Fig. 2c). This strongly supports the brighter appearance of edge features in SEM images as surface morphology induced effects in agreement with the roughening hypothesis in vacuum-only and gaseous nitrogen ambient pressure experiments, mentioned before. When EDX is performed on the dendritic 3D structures obtained at a bias voltage to 80 V, a massive but sole increase of the carbon signal is detected (red line in Fig. 2f), which clearly identifies the 3D structure as carbon feature. We assume that this effect is due to a voltage dependent discharge effect in the localized high-pressure region of naphthalene, which explains the dendritic morphology between the substrate and the AFM tip.

Finally, we aimed on the exclusion of the deposition component during TEBI processing by implementing gaseous CO_2. Due to technical reasons, related to the vacuum system, we changed to ambient pressure conditions and repeated the TEBI experiment. As evidently shown in the SEM image overview in Fig. 3a, the results look very similar to the carbonaceous precursor naphthalene but with a material removal onset at higher voltages.

As for naphthalene-based TEBI processing, we again conducted successive AFM measurements at selected lines (indicated in Fig. 3a), shown in Fig. 3b by 3D height images (left) and related cross-sectional profiles (right). The narrow lines for 40 V do evidently not show any height increase but in contrary only a sub-10 nm deep trench that clearly reveals CO_2-TEBI processing to be a material removal process in this case. For increased voltages, the trenches get deeper, as shown for the 80 V line in purple, but again possess the M-shaped cross-sectional shapes as qualitatively also observed for naphthalene-based TEBI processing (Fig. 2e).

Before an interpretation attempt of this special morphology can be given, we present according EDX data, summarized for two selected etch-lines in Fig. 3c. Here it becomes evident that the gold signals (blue) are clearly decreasing at the trench regions, while the silicon signals increase in intensity (purple). Nevertheless, what is even more important is the stable carbon signal across both presented lines, as indicated by the orange curve in Fig. 3c. This strongly suggests that even the slightly elevated edge features, detected by AFM (Fig. 3b), are solely composed of gold, which again substantiates the hypothesis of a gold roughening prior the actual material removal sets. This can also presumably explain the M-shaped features for accordingly high voltages, when considering a laterally decaying electric field due to the divergent emission characteristics starting at the very tip apex. In this case, the center regions are already in the material removal mode, while the outmost regions reveal the initial roughening mode prior to the removal of material. The same argumentation holds for naphthalene-based TEBI processing and for the vacuum-only TEBI experiments, although the latter is strongly dependent on the local contamination situation, while the former provides more stable gas conditions.

The downside for CO_2-based TEBI processing at ambient pressures is however, the clearly higher line edge roughness, which might be a consequence of the very high local pressures as well as a currently unavoidable spatial distribution of electrons during their tip emission. Although localized material deposition and removal was clearly demonstrated using scanning probes, the above-discussed results must be considered only as a starting point for further technological exploration in comparison to the existing alternatives and the addressed system needs. Further studies are hence indispensable to determine, for instance, the optimum pressure range for high-quality material removal results [17] and to create an improved overall understanding of TEBI processing.

4. Summary

In summary, we demonstrated first results of tip enhanced electron beam induced (TEBI) processing with respect to the deposition of 3D carbon features and the removal of gold from the surface. The study suggests for the deposition a mechanism similar to focused electron beam induced deposition, but without an indispensably needed vacuum. From experiments with different gases (e.g., air, nitrogen) and chamber pressure conditions, we deduced that the use of gaseous CO_2 as a process gas enables tip-based removal of gold from the surface. It is noteworthy here that despite the presence of CO_2, material removal occurs without the deposition of carbon, as was observed in contrast with the use of naphthalene- based TEBI processing. Even without a deep optimization of local pressure, scanning speed as well as bias voltage, the experiments showed that comparable or predictable results including, for instance, line edge roughness, trench width and depth are successfully achieved. This study thus provides a first cornerstone for an intriguing technology for future micro- and nanoscale device fabrication with the unique

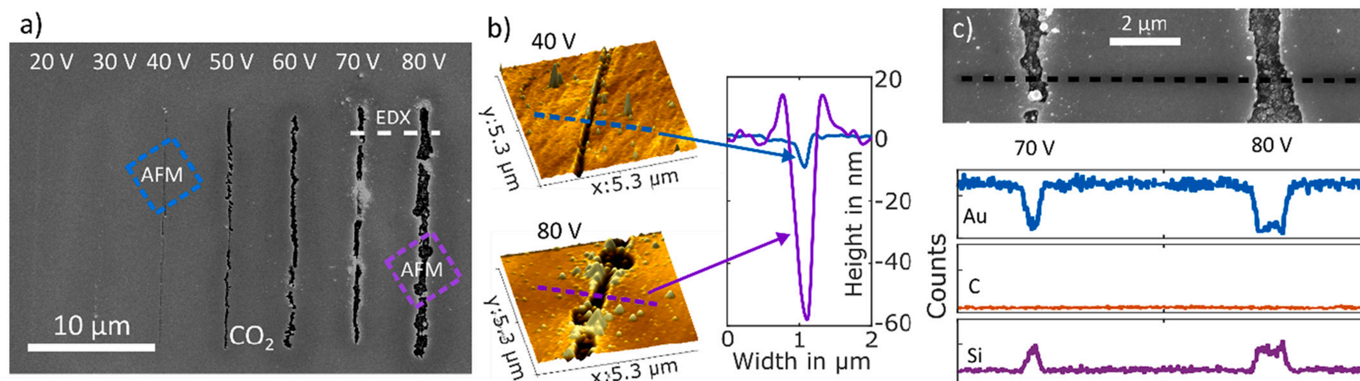

Fig. 3. a) Surface image after TEBI processing of a line pattern (line length 20 µm) in a CO_2 atmosphere at ambient pressure using a bias voltage of 20 V to 80 V at an emission current and writing speed of 180 pA and 0.05 µm/s, respectively. b) AFM image of selected sections and lines (40 V and 80 V bias voltage) as well as an exemplary cross-section profile. Scanned areas are indicated by dashed squares in a). The etched trench width and depth increase with increasing bias voltage. Using, for instance, 40 V bias voltage yield a trench with 200 nm in width and a depth of 10 nm. c) SEM/EDX line scan analysis of the substrate a lines created at 70 V and 80 V bias voltage. The line scan was carried out at sample position indicated in a). The count axis is the same for all elements. The EDX signal shows furthermore clearly that the top gold was etched during the line pattern creation. Notable carbonaceous deposits were not detected. (For interpretation of the references to colour in this figure legend, the reader is referred to the web version of this article.)

possibility of a cyclic workflow between modification and inspection for true rapid prototyping.

Declaration of Competing Interest

The authors declare that they have no known competing financial interests or personal relationships that could have appeared to influence the work reported in this paper.

Acknowledgements

We sincerely thank the Vector Foundation (grant number P2018-0133) for financial support, nano analytik GmbH for lending the AFMinSEM device for the experiments, and the Center of Micro- and Nanotechnologies (TU Ilmenau) for their overall support.

References

[1] D. Andrews, T. Nann, R.H. Lipson (Eds.), Comprehensive nanoscience and nanotechnology, 2nd ed., Elsevier Science & Technology, San Diego, 2019.
[2] J. Chen, K. Xu, Applications of atomic force microscopy in materials, semiconductors, polymers, and medicine: a minireview, Instrument Sci Technol 48 (2020) 667–681, https://doi.org/10.1080/10739149.2020.1764030.
[3] R. Garcia, A.W. Knoll, E. Riedo, Advanced scanning probe lithography, Nat Nanotechnol 9 (2014) 577–587, https://doi.org/10.1038/nnano.2014.157.
[4] M. Hofmann, C. Lenk, T. Ivanov, I.W. Rangelow, A. Reum, A. Ahmad, M. Holz, E. Manske, Field emission from diamond nanotips for scanning probe lithography, J Vac Sci Technol B 36 (2018) 06JL02, https://doi.org/10.1116/1.5048193.
[5] J.N. Randall, J.H.G. Owen, J. Lake, E. Fuchs, Next generation of extreme-resolution electron beam lithography, J Vacuum Sci Technol B Nanotechnol Microelectron Mater Process Measure Phenom 37 (2019) 61605, https://doi.org/10.1116/1.5119392.
[6] A.I. Dago, S. Sangiao, R. Fernández-Pacheco, J.M. de Teresa, R. Garcia, Chemical and structural analysis of sub-20 nm graphene patterns generated by scanning probe lithography, Carbon 129 (2018) 281–285, https://doi.org/10.1016/j.carbon.2017.12.033.
[7] H. Wolf, C. Rawlings, P. Mensch, J.L. Hedrick, D.J. Coady, U. Duerig, A.W. Knoll, Sub-20 nm silicon patterning and metal lift-off using thermal scanning probe lithography, J Vac Sci Technol B 33 (2015) 02B102, https://doi.org/10.1116/1.4901413.
[8] M. Holz, C. Reuter, A. Ahmad, A. Reum, M. Hofmann, T. Ivanov, I.W. Rangelow, Correlative microscopy and nanofabrication with AFM integrated with SEM, Micros Today 27 (2019) 24–30, https://doi.org/10.1017/S1551929519001068.
[9] I. Utke, Nanofabrication using focused ion and electron beams: principles and applications, Oxford University Press Incorporated, Cary, 2011.
[10] M. Huth, F. Porrati, S. Barth, Living up to its potential—direct-write nanofabrication with focused electron beams, J Appl Phys 130 (2021), 170901, https://doi.org/10.1063/5.0064764.
[11] R. Garcia, N.S. Losilla, J. Martínez, R.V. Martinez, F.J. Palomares, Y. Huttel, M. Calvaresi, F. Zerbetto, Nanopatterning of carbonaceous structures by field-induced carbon dioxide splitting with a force microscope, Appl Phys Lett 96 (2010), 143110, https://doi.org/10.1063/1.3374885.
[12] I.W. Rangelow, T. Ivanov, A. Ahmad, M. Kaestner, C. Lenk, I.S. Bozchalooi, F. Xia, K. Youcef-Toumi, M. Holz, A. Reum, Review article: active scanning probes: a versatile toolkit for fast imaging and emerging nanofabrication, J Vacuum Sci Technol B Nanotechnol Microelectron Mater Process Measure Phenom 35 (2017) 06G101, https://doi.org/10.1116/1.4992073.
[13] S. Lenk, M. Kaestner, C. Lenk, T. Angelov, Y. Krivoshapkina, I.W. Rangelow, 2D simulation of Fowler-Nordheim Electron emission in scanning probe lithography, J Nanomater Mol Nanotechnol 06 (2016), https://doi.org/10.4172/2324-8777.1000201.
[14] S. Barth, M. Huth, F. Jungwirth, Precursors for direct-write nanofabrication with electrons, J Mater Chem C 8 (2020) 15884–15919, https://doi.org/10.1039/D0TC03689G.
[15] A.E. Vladár, K.P. Purushotham, M.T. Postek, Contamination specification for dimensional metrology SEMs, in: Metrology, inspection, and process control for microlithography XXII, California, USA, SPIE, San Jose, 2008, p. 692217.
[16] M. Kaestner, I.W. Rangelow, Scanning probe lithography on calixarene towards single-digit nanometer fabrication, Int J Extrem Manuf 2 (2020) 32005, https://doi.org/10.1088/2631-7990/aba2d8.
[17] C. Kong, S. Cheong, R.D. Tilley, Recent development in focused ion beam nanofabrication, in: D. Andrews, T. Nann, R.H. Lipson (Eds.), Comprehensive nanoscience and nanotechnology, 2nd ed., Elsevier Science & Technology, San Diego, 2019, pp. 327–356.